Combined Homogeneous and Heterogeneous Hydrogenation with Parahydrogen to Yield Catalyst-Free Solutions of Hyperpolarized [1-^{13}C]Succinate

James Eills,[*,†,‡,¶] Román Picazo-Frutos,[‡,¶] Dudari B. Burueva,[§] Larisa M. Kovtunova,[§,‖,⊥] Marc Azagra,[†] Irene Marco-Rius,[†] Dmitry Budker,[#,‡,¶,#] and Igor V. Koptyug[*,§]

†*Institute for Bioengineering of Catalonia, Barcelona Institute of Science and Technology, 08028 Barcelona, Spain*

‡*Helmholtz-Institut Mainz, GSI Helmholtzzentrum für Schwerionenforschung, 55128 Mainz, Germany*

¶*Institute for Physics, Johannes Gutenberg-Universität Mainz, 55099 Mainz, Germany*

§*International Tomography Center SB RAS, 3A Institutskaya St., Novosibirsk 630090, Russia*

‖*Novosibirsk State University, 2 Pirogova St., Novosibirsk 630090, Russia*

⊥*Boreskov Institute of Catalysis SB RAS, 5 Acad. Lavrentiev Ave., Novosibirsk 630090, Russia*

#*Department of Physics, University of California, Berkeley, CA 94720-7300 USA*

Received April 19, 2023; E-mail: jeills@ibecbarcelona.eu; koptyug@tomo.nsc.ru

Abstract: We show that catalyst-free aqueous solutions of hyperpolarized [1-^{13}C]succinate can be produced using parahydrogen-induced polarization (PHIP) and a combination of homogeneous and heterogeneous catalytic hydrogenation reactions. We generate hyperpolarized [1-^{13}C]fumarate at 23% ^{13}C polarization via PHIP with a homogeneous ruthenium catalyst, and subsequently remove the toxic catalyst and reaction side products via a purification procedure. Following this, we perform a second hydrogenation reaction to convert the fumarate into succinate using a solid Pd/Al_2O_3 catalyst. The catalyst is filtered off to yield a clean aqueous solution containing [1-^{13}C]succinate at 11.9% ^{13}C polarization for the hyperpolarized molecules. In this proof-of-principle demonstration we simplified the purification procedure by adding unpolarized fumarate to the mixtures so the observed succinate polarization was lower, but this step is not necessary for applications. This inexpensive polarization protocol has a turnover time of a few minutes, and represents a major advance for in vivo applications of [1-^{13}C]succinate as a hyperpolarized contrast agent.

Hyperpolarization-enhanced magnetic resonance imaging (MRI) and spectroscopy (MRS) allows clinicians to track metabolic processes noninvasively in real time in the body.[1,2] Parahydrogen-induced polarization (PHIP) has emerged as an inexpensive contrast-agent hyperpolarization method.[3–11] Parahydrogen (p-H_2) can be readily prepared by cooling hydrogen gas to $\lesssim$30 K, and then catalytically reacted with an unsaturated precursor to produce a hyperpolarized product molecule.[12,13] The hyperpolarization is transferred to a ^{13}C spin in the molecule,[14–20] and then the hyperpolarized molecule can be injected for in vivo imaging,[15,21,22] and more recent work has allowed for purification prior to injection.[23] PHIP relies on chemically-specific hydrogenation reactions, often carried out in an organic solvent using an organometallic catalyst. Since the product molecule must be purified and extracted into an aqueous solution, the number of targets that can be produced in this way is limited. To date only [1-^{13}C]pyruvate and [1-^{13}C]fumarate have been hyperpolarized via PHIP and then purified to a sufficient level for safe in vivo application.[9,23]

Another promising contrast agent is [1-^{13}C]succinate, which has been used for real-time in vivo tumor detection[24] and as a marker for stroke-affected regions of the brain.[25] [1-^{13}C]succinate-d_2 has been produced at high ^{13}C polarization levels via PHIP by hydrogenating [1-^{13}C]acetylene dicarboxylate or [1-^{13}C]fumarate-d_2 in aqueous solution,[24,26–30] and studied in vivo as a contrast agent,[24,27,28] but in these demonstrations the toxic catalyst remained in the solutions. In an exciting piece of work, [1-^{13}C]maleic anhydride-d_2 was hydrogenated with p-H_2 in $CDCl_3$ to produce [1-^{13}C]succinic anhydride-d_2, which was hydrolyzed with NaOD to yield [1-^{13}C]succinate in the aqueous phase, leaving the catalyst in the organic $CDCl_3$ phase.[31] However, the concentration and polarization of succinate in the aqueous phase were not reported, and the hydrogenation yield was 40%, meaning 60% of the initial maleic anhydride was likely hydrolyzed to toxic maleate, contaminating the succinate solution.

In contrast to homogeneous catalysis, removal of the catalyst is much easier after a heterogeneous catalytic process since the catalyst and the products represent different phases. Heterogeneous catalysts have been demonstrated to produce PHIP effects.[32–34] However, this approach is generally inferior to homogeneous hydrogenation in terms of achievable polarization levels (often, 1-3% or even less) since the p-H_2-derived atoms can migrate across the catalyst surface and lose their correlated spin state (and hence polarization). Hydrogen atom mobility can be suppressed by poisoning the catalyst surface,[35,36] or by moving to supported-metal catalysts with smaller active sites[32,37] or even single-atom solid catalysts,[38,39] but this comes at the cost of catalytic activity.

In this work we leverage the advantages of both homogeneous and heterogeneous catalysis to produce hyperpolarized [1-^{13}C]succinate. We employ an established method to hyperpolarize [1-^{13}C]fumarate via homogeneous PHIP, yielding the pure molecule in aqueous solution at >20% ^{13}C polarization.[9] From this point, a heterogeneous hydrogenation catalyst is used to facilitate a second hydrogenation step to produce hyperpolarized [1-^{13}C]succinate, and the ^{13}C polarization survives this process.

This manuscript is based on work done prior to February 24, 2022.

Measuring the performance of the heterogeneous catalyst

For the hydrogenation of fumarate to succinate, we tested a number of heterogeneous catalysts. 20-30 mg of the catalyst was loaded into a pressurizable 5 mm NMR tube containing 500 μL of 100 mM sodium fumarate in D_2O, and the sample was heated to a fixed temperature. Hydrogen gas (not para-enriched) was then bubbled through the solution at 6 bar to initiate the reaction. After 30 s, the tube was depressurized and the solution was extracted from the NMR tube and filtered to remove the catalyst. High-field ^{1}H NMR spectra were acquired from the samples. The experiments and results are summarized in Table 1.

Table 1. Summary of hydrogenation experiments employing different heterogeneous catalysts and experimental conditions to transform 100 mM sodium fumarate in D_2O into succinate.

Catalyst	Loading (mg)	T (°C)	Bubbling rate (mL/min)	Yield (%)
Pt/Al_2O_3	20	90	80	32
Pd/C	20	90	80	66
Pd/Al_2O_3	20	90	80	70
	20	90	120	85
	30	98	150	98

From the ^{1}H NMR spectra we were able to quantify the fumarate and succinate concentrations, and hence determine the reaction yield. Pd/Al_2O_3 performed best and was selected for following experiments due to good powder properties (wettability, flowability, and chemical stability). The ^{1}H NMR spectra for the three reactions using Pd/Al_2O_3 are shown in Fig. 1. From these spectra we were unable to detect any reaction side-products (e.g., the *cis*-isomer maleate, or hydrogenolysis products from C-C or C-O bond scission), indicating excellent reaction selectivity. For all subsequent experiments, we used (unless otherwise specified) 15 wt.% Pd supported on Al_2O_3 as the heterogeneous catalyst. See Supporting Information for catalyst characterization data.

Forming hyperpolarized succinate

Hydrogenation of acetylene dicarboxylate was carried out using parahydrogen and a homogeneous catalyst ([RuCp*(MeCN)3]PF_6) in D_2O to produce fumarate with the protons in a hyperpolarized state. 2.2% of the fumarate molecules are the naturally-occurring [1-^{13}C]isotopomer, and a magnetic field cycle[20] was applied to the sample to transfer the proton hyperpolarization to the ^{13}C nucleus in those molecules. 200-250 μL of this solution was taken (Sample A) and placed in a 1.4 T benchtop NMR magnet for ^{13}C signal acquisition. The average [1-^{13}C]fumarate concentration in this sample was 43 ± 5 mM, and the ^{13}C polarization was 23 ± 2%. The remainder of the hyperpolarized fumarate sample underwent a purification procedure: we mixed the hyperpolarized fumarate solution with 370 ± 20 μL of a 1 M disodium fumarate in D_2O solution (to raise the overall fumarate concentration in order to speed up the precipitation step), and HCl was added to the sample to induce precipitation of solid fumaric acid. The remaining reaction solution was vacuum-filtered off. The fumaric acid crystals were redissolved in 1 mL of 1 M NaOD in D_2O (unless otherwise specified) to yield a clean aqueous solution of ^{13}C-polarized [1-^{13}C]fumarate (Sample B).

Sample B was injected into a second hydrogenation reactor (Reactor 2) held at 85°C, pre-loaded with 15 wt.% Pd/Al_2O_3 powder. Hydrogen gas was bubbled through the mixture at 6 L/min and a pressure of 8.5 bar for 20 s. A two-way valve was opened to release the solution into a 5 mm NMR tube beneath Reactor 2, and the solid catalyst was caught in a 1/8 in. capillary directly above two-way valve (because the valve inner diameter was smaller than the catalyst pellets), yielding clean aqueous succinate solutions. The 5 mm NMR tube containing Sample B was placed in the 1.4 T benchtop NMR magnet for signal acquisition. The experimental apparatus is shown in Fig. 2, and experimental details are provided in the Supplementary Information.

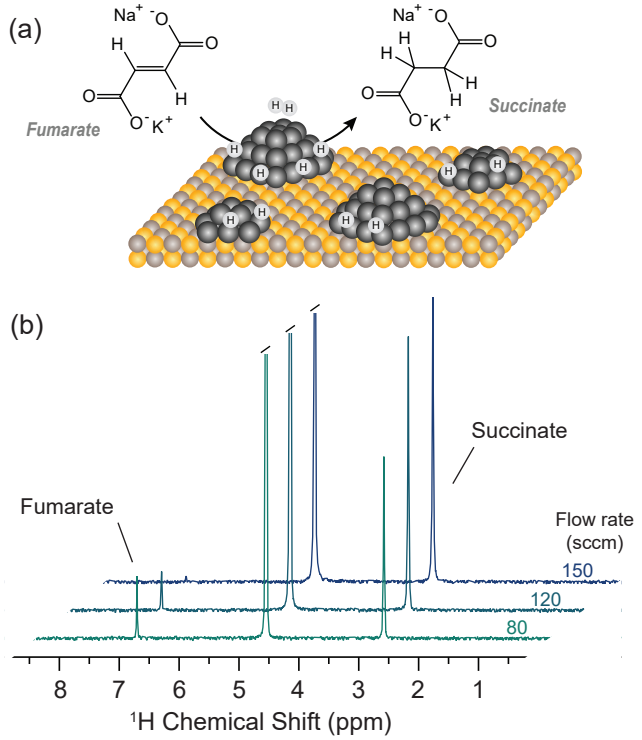

Figure 1. (a) The heterogeneously-catalyzed hydrogenation of fumarate to succinate. The yellow and grey balls represents alumina, and the black balls represent palladium atoms. (b) ^{1}H NMR spectra of three separate reaction solutions after bubbling H_2 through 100 mM disodium fumarate in D_2O over 20 wt.% Pd/Al_2O_3 catalyst. These three spectra correspond to the last three rows of Table 1. Higher H_2 bubbling rate resulted in more succinate being formed, and no side products were observed. The peak at 4.6 ppm is from the residual protons in D_2O. Further experimental conditions are provided in Table 1.

The complete procedure described above was repeated six times with different amounts of Pd/Al_2O_3 present. The [1-^{13}C]fumarate and [1-^{13}C]succinate polarizations and reaction yields are shown in Fig. 3(a). The average concentration of fumarate in the sample prior to the fumarate → succinate hydrogenation was 180±40 mM. The polarizations reported are those of the molecules in solution that underwent the hyperpolarization process, discounting the unpolarized molecules added during the purification process (see Supplementary Information). Reactor 2 was not cleaned between experiments, meaning there was residual heterogeneous catalyst left after each run: note that in Run 5 no new heterogeneous catalyst was added to the reactor, but the reaction yield was still 8.0%.

The procedure was repeated another four times to investigate the effect of solution pH. The solution used to redissolve the purified fumaric acid was at 0.5 M NaOD concentration

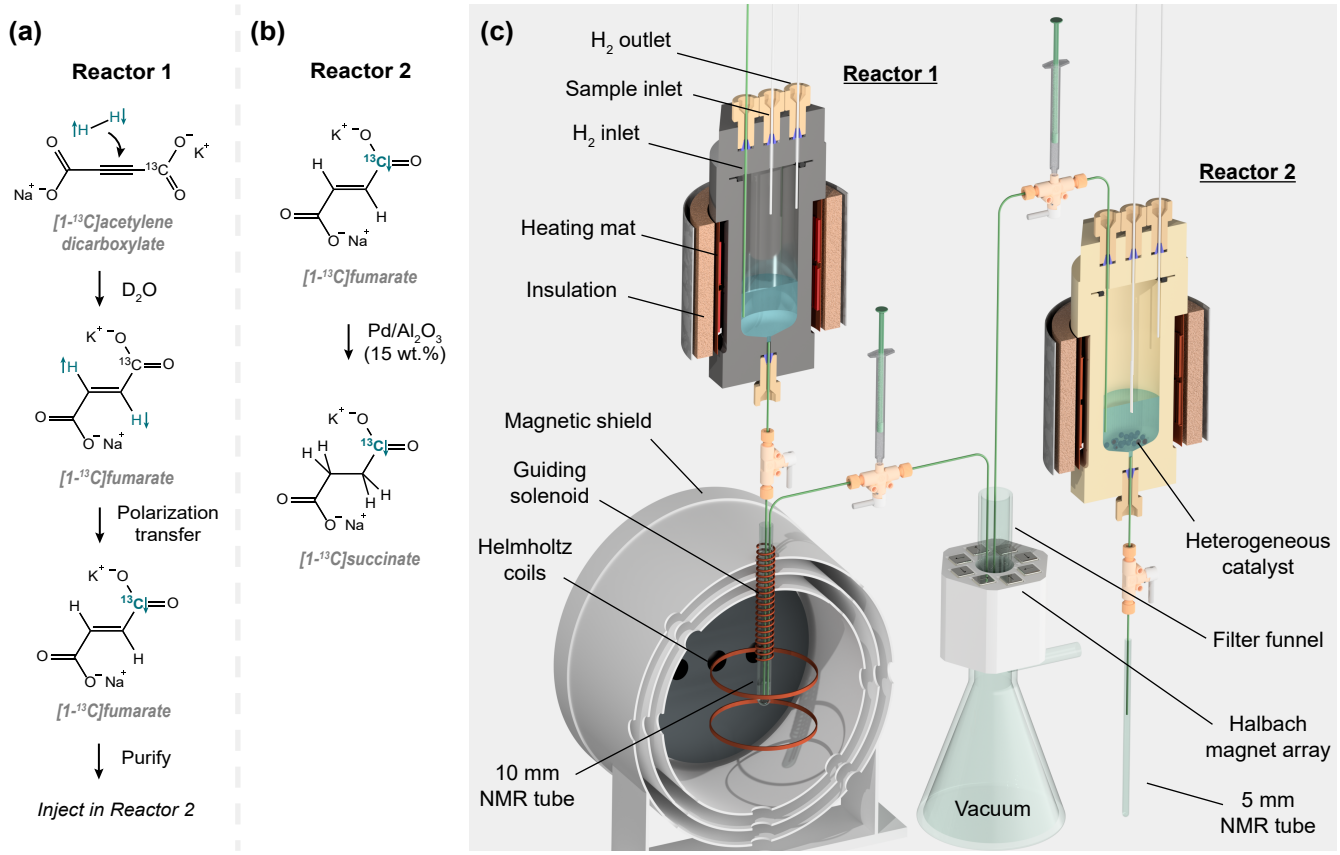

Figure 2. (a) The formation of purified hyperpolarized fumarate solutions. (b) The formation of succinate by hydrogenating fumarate in Reactor 2. (c) The apparatus used for the succinate hyperpolarization procedure described in the main text.

for the first two runs, and 0.2 M NaOD concentration for the next two, yielding reaction solutions with pH 14 and pH 3, respectively. The results are shown in Fig. 3(b). The ^{13}C polarization of both [1-^{13}C]fumarate and [1-^{13}C]succinate is an order of magnitude lower when the reaction solution is acidic. The reason for this is subject to ongoing investigation.

An experiment was carried out as described before, but with 22% ^{13}C enrichment in the [1-^{13}C] position of the acetylene dicarboxylate. The resulting ^{13}C NMR spectrum of the hyperpolarized reaction solution is shown in Fig. 3(c) alongside a thermal equilibrium ^{13}C spectrum of a 500 mM ^{13}C-labelled standard, also acquired at 1.4 T. The ^{13}C polarization of the hyperpolarized [1-^{13}C]succinate molecules was measured to be 11.9%. The polarization is higher than the results in Fig. 3a because the sample purification and transport steps were faster. The ^{13}C T_1 times of [1-^{13}C]fumarate and [1-^{13}C]succinate in the purified aqueous solution (at pH 14) were measured at 1.4 T by pulsing every 7.2 s with a 5° flip-angle pulse. The results are plotted in Fig. 3d.

Our results show that this two-step hydrogenation is a viable method for the production of hyperpolarized [1-^{13}C]succinate for biological applications. The [1-^{13}C]succinate ^{13}C polarization is consistently lower than that of [1-^{13}C]fumarate, likely due to a relaxation process. This may be a catalyst-surface effect, or a solution-state T_1 difference at the lower fields experienced during hydrogenation and sample transport.

For the fumarate purification we mixed the hyperpolarized fumarate solution with a solution of 1 M unpolarized fumarate to raise the overall concentration to speed up the precipitation step. This is not necessary if higher hydrogen gas pressure and starting material concentration are used, to form fumarate in $\gtrsim$200 mM concentration to allow direct precipitation from the reaction solution.[40]

In high resolution ^{1}H NMR spectra we observed that the succinate formed was partially deuterated during the heterogeneous hydrogenation reaction (i.e., while the sample was in the presence of the heterogeneous catalyst). We carried out six additional 30 s hydrogenation experiments at 90°C using 10, 15, and 20 wt.% Pd/Al_2O_3, and observed 16.5±1.5% deuteration of the succinate: 43% succinate-h_4, 50% succinate-d_1 and 8% succinate-2,3-d_2. This would lead to an underestimation of the succinate concentration measured by ^{1}H NMR, so we corrected for this factor in all results (including in Table 1). The fumarate→succinate hydrogenation could be carried out with D_2 to produce succinate-2,3-d_2 which may increase the succinate ^{13}C T_1.

The fumarate→succinate yield in Reactor 2 was consistently lower than in experiments carried out in a 5 mm NMR tube. We believe this is because in the reactor the catalyst particles were not well-agitated during hydrogen bubbling. Higher succinate yields should be readily achievable by employing a more optimized reaction vessel. For some applications it may be desirable to not hydrogenate fumarate fully, so that the final solution contains two hyperpolarized probe molecules for multi-component studies.[41] Otherwise, fumarate spectral peaks could be removed by achieving 100% yield, or simply saturating the fumarate ^{13}C signals with rf pulses.

In other work using hyperpolarized succinate, the diethyl ester form has been employed which permeates cell mem-

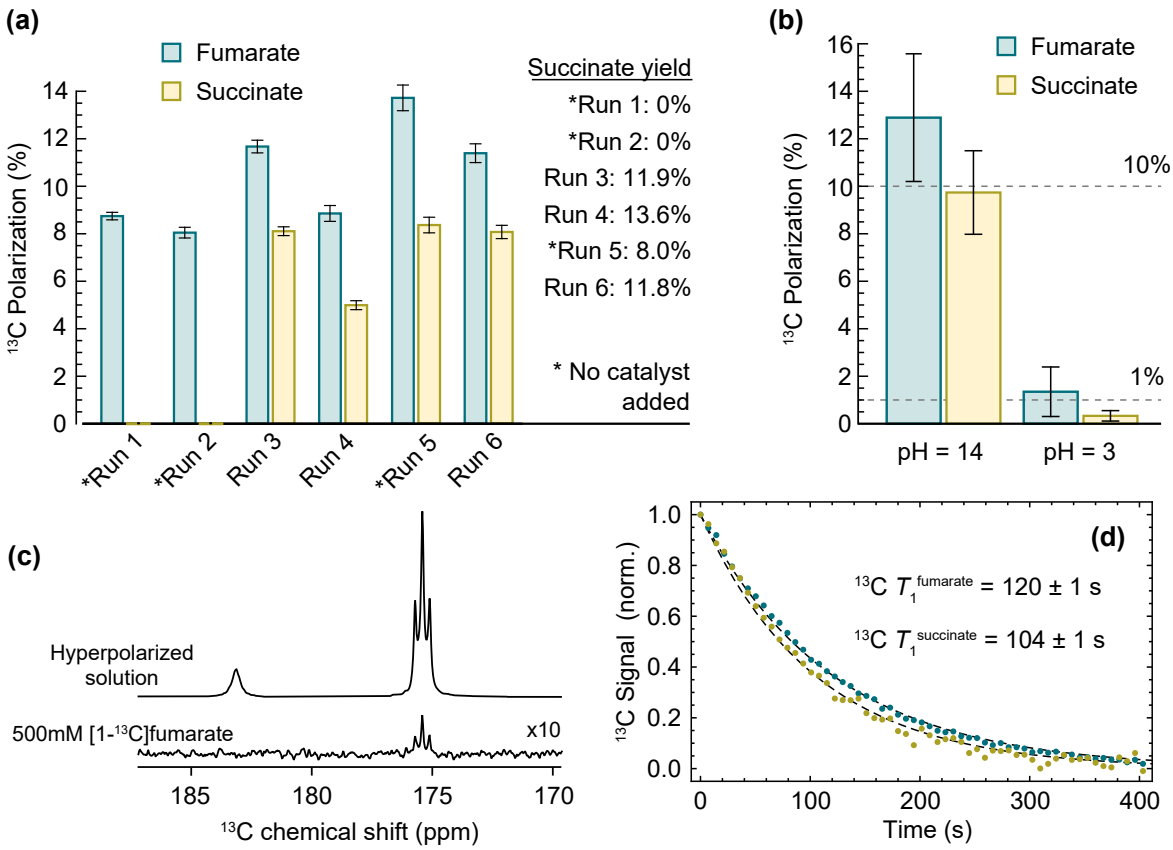

Figure 3. (a) ^{13}C polarization of [1-^{13}C]fumarate and [1-^{13}C]succinate for a series of experiments performed in succession. The mass of heterogeneous catalyst added to Reactor 2 was 0, 0, 47, 62, 0, 52 mg for Runs 1 to 6, and the reactor was not cleaned between experiments. The error bars indicate the error on polarization from the propagated experimental uncertainty of the sample volumes. (b) ^{13}C polarization of [1-^{13}C]fumarate and [1-^{13}C]succinate for experiments in which the fumarate → succinate hydrogenation was carried out in solutions at different pH. Two replicates were performed for the two cases (high and low pH hydrogenation) and the error bars represent the standard error of the measurements. (c) A comparison between ^{13}C NMR spectra of a hyperpolarized reaction solution at 22% ^{13}C-labelling of the fumarate and succinate, and a thermal-equilibrium standard of 100% ^{13}C-labelled [1-^{13}C]fumarate at 500 mM concentration. The hyperpolarized spectrum was acquired with a 30° flip-angle pulse, and the thermal-equilibrium spectrum was acquired with a 90° flip-angle pulse. Both spectra are shown with 0.5 Hz line broadening. The succinate ^{13}C polarization (accounting for the excitation pulse flip-angle difference) was 11.9% and the succinate yield was 16.8%. (d) ^{13}C T_1 relaxation of the hyperpolarized fumarate (teal) and succinate (yellow) signals at 1.4 T. The signals were excited with a 5° flip-angle pulse every 7.2 s, and the data points represent the integrals of the resulting [1-^{13}C] NMR peaks.

branes faster.[28,42] Diethyl succinate cannot be produced with the method we show here because diethyl fumarate cannot be purified in the same way as fumaric acid, although it may be possible to carry out a rapid esterification on the purified succinate.

In this work we have demonstrated a novel, inexpensive method to produce catalyst-free hyperpolarized succinate via PHIP. We achieve 11.9% ^{13}C polarization in hyperpolarized succinate molecules, which is high-enough for in vivo applications. The heterogeneous catalyst employed (Pd/Al_2O_3) showed 100% selectivity for fumarate→succinate conversion, and we do not detect side products or contaminants in the succinate solutions. We believe this work marks an exciting new class of hyperpolarization experiments in which a rapid chemical synthesis/modification is carried out on a purified hyperpolarized molecule to produce a new contrast agent.

References

(1) Eills, J.; Budker, D.; Cavagnero, S.; Chekmenev, E. Y.; Elliott, S. J.; Jannin, S.; Lesage, A.; Matysik, J.; Meersmann, T.; Prisner, T.; Reimer, J. A.; Yang, H.; Koptyug, I. V. Spin Hyperpolarization in Modern Magnetic Resonance. *Chem. Rev.* **2023**, *123*, 1417–1551.

(2) Nelson, S. J.; Kurhanewicz, J.; Vigneron, D. B.; Larson, P. E.; Harzstark, A. L.; Ferrone, M.; Van Criekinge, M.; Chang, J. W.; Bok, R.; Park, I., et al. Metabolic imaging of patients with prostate cancer using hyperpolarized [1-^{13}C] pyruvate. *Sci. Transl. Med.* **2013**, *5*, 198ra108–198ra108.

(3) Hövener, J.-B.; Pravdivtsev, A. N.; Kidd, B.; Bowers, C. R.; Glöggler, S.; Kovtunov, K. V.; Plaumann, M.; Katz-Brull, R.; Buckenmaier, K.; Jerschow, A., et al. Parahydrogen-based hyperpolarization for biomedicine. *Angew. Chem. Int. Ed* **2018**, *57*, 11140–11162.

(4) Golman, K.; Axelsson, O.; Jóhannesson, H.; Månsson, S.; Olofsson, C.; Petersson, J. Parahydrogen-induced polarization in imaging: Subsecond ^{13}C angiography. *Magn. Reson. Med.* **2001**, *46*, 1–5.

(5) Reineri, F.; Boi, T.; Aime, S. Parahydrogen induced polarization of ^{13}C carboxylate resonance in acetate and pyruvate. *Nat. Commun.* **2015**, *6*, 1–6.

(6) Korchak, S.; Emondts, M.; Mamone, S.; Blümich, B.; Glöggler, S. Production of highly concentrated and hyperpolarized metabolites within seconds in high and low magnetic fields. *Phys. Chem. Chem. Phys.* **2019**, *21*, 22849–22856.

(7) Eills, J.; Cavallari, E.; Carrera, C.; Budker, D.; Aime, S.; Reineri, F. Real-Time Nuclear Magnetic Resonance Detection of Fumarase Activity Using Parahydrogen-Hyperpolarized [1-^{13}C] Fumarate. *J. Am. Chem. Soc.* **2019**, *141*, 20209–20214.

(8) Dagys, L.; Jagtap, A. P.; Korchak, S.; Mamone, S.; Saul, P.; Levitt, M. H.; Glöggler, S. Nuclear hyperpolarization of (1-^{13}C)-pyruvate in aqueous solution by proton-relayed side-arm hydrogenation. *Analyst* **2021**, *146*, 1772–1778.

(9) Knecht, S.; Blanchard, J. W.; Barskiy, D.; Cavallari, E.; Dagys, L.; Van Dyke, E.; Tsukanov, M.; Bliemel, B.; Münne-

mann, K.; Aime, S., et al. Rapid hyperpolarization and purification of the metabolite fumarate in aqueous solution. *Proc. Natl. Acad. Sci. U.S.A.* **2021**, *118*.
(10) Hale, W. G.; Zhao, T. Y.; Choi, D.; Ferrer, M.-J.; Song, B.; Zhao, H.; Hagelin-Weaver, H. E.; Bowers, C. R. Toward Continuous-Flow Hyperpolarisation of Metabolites via Heterogenous Catalysis, Side-Arm-Hydrogenation, and Membrane Dissolution of Parahydrogen. *ChemPhysChem* **2021**, *22*, 822–827.
(11) Mamone, S.; Jagtap, A. P.; Korchak, S.; Ding, Y.; Sternkopf, S.; Glöggler, S. A Field-Independent Method for the Rapid Generation of Hyperpolarized [1-13C]Pyruvate in Clean Water Solutions for Biomedical Applications. *Angewandte Chemie International Edition* **2022**, *61*, e202206298.
(12) Bowers, C. R.; Weitekamp, D. P. Parahydrogen and synthesis allow dramatically enhanced nuclear alignment. *J. Am. Chem. Soc.* **1987**, *109*, 5541–5542.
(13) Schmidt, A. B.; Bowers, C. R.; Buckenmaier, K.; Chekmenev, E. Y.; de Maissin, H.; Eills, J.; Ellermann, F.; Glöggler, S.; Gordon, J. W.; Knecht, S., et al. Instrumentation for Hydrogenative Parahydrogen-Based Hyperpolarization Techniques. *Anal. Chem.* **2022**, *94*, 479–502.
(14) Goldman, M.; Jóhannesson, H. Conversion of a proton pair para order into 13C polarization by rf irradiation, for use in MRI. *Comptes Rendus Physique* **2005**, *6*, 575–581, Aircraft trailing vortices.
(15) Goldman, M.; Jóhannesson, H.; Axelsson, O.; Karlsson, M. Hyperpolarization of 13C through order transfer from parahydrogen: A new contrast agent for MRI. *Magnetic Resonance Imaging* **2005**, *23*, 153–157, Proceedings of the Seventh International Conference on Recent Advances in MR Applications to Porous Media.
(16) Eills, J.; Stevanato, G.; Bengs, C.; Glöggler, S.; Elliott, S. J.; Alonso-Valdesueiro, J.; Pileio, G.; Levitt, M. H. Singlet order conversion and parahydrogen-induced hyperpolarization of ^{13}C nuclei in near-equivalent spin systems. *J. Magn. Reson.* **2017**, *274*, 163–172.
(17) Eills, J.; Blanchard, J. W.; Wu, T.; Bengs, C.; Hollenbach, J.; Budker, D.; Levitt, M. H. Polarization transfer via field sweeping in parahydrogen-enhanced nuclear magnetic resonance. *J. Chem. Phys.* **2019**, *150*, 174202.
(18) Emondts, M.; Colell, J. F. P.; Blümich, B.; Schleker, P. P. M. Polarization transfer efficiency in PHIP experiments. *Phys. Chem. Chem. Phys.* **2017**, *19*, 21933–21937.
(19) Rodin, B. A.; Kozinenko, V. P.; Kiryutin, A. S.; Yurkovskaya, A. V.; Eills, J.; Ivanov, K. L. Constant-adiabaticity pulse schemes for manipulating singlet order in 3-spin systems with weak magnetic non-equivalence. *Journal of Magnetic Resonance* **2021**, *327*, 106978.
(20) Rodin, B. A.; Eills, J.; Picazo-Frutos, R.; Sheberstov, K. F.; Budker, D.; Ivanov, K. L. Constant-adiabaticity ultralow magnetic field manipulations of parahydrogen-induced polarization: application to an AA'X spin system. *Phys. Chem. Chem. Phys.* **2021**, *23*, 7125–7134.
(21) Bhattacharya, P.; Chekmenev, E. Y.; Reynolds, W. F.; Wagner, S.; Zacharias, N.; Chan, H. R.; Bünger, R.; Ross, B. D. Parahydrogen-induced polarization (PHIP) hyperpolarized MR receptor imaging in vivo: a pilot study of 13C imaging of atheroma in mice. *NMR in Biomedicine* **2011**, *24*, 1023–1028.
(22) Schmidt, A. B.; Berner, S.; Braig, M.; Zimmermann, M.; Hennig, J.; von Elverfeldt, D.; Hövener, J.-B. In vivo 13C-MRI using SAMBADENA. *PLOS ONE* **2018**, *13*, 1–15.
(23) Cavallari, E.; Carrera, C.; Sorge, M.; Bonne, G.; Muchir, A.; Aime, S.; Reineri, F. The 13C hyperpolarized pyruvate generated by ParaHydrogen detects the response of the heart to altered metabolism in real time. *Sci. Rep.* **2018**, *8*, 1–9.
(24) Zacharias, N. M.; McCullough, C. R.; Wagner, S.; Sailasuta, N.; Chan, H. R.; Lee, Y.; Hu, J.; Perman, W. H.; Henneberg, C.; Ross, B. D., et al. Towards real-time metabolic profiling of cancer with hyperpolarized succinate. *J. Mol. Imaging Dyn.* **2016**, *6*, 1000123.
(25) Ross, B.; Bhattacharya, P.; Wagner, S.; Tran, T.; Sailasuta, N. Hyperpolarized MR Imaging: Neurologic Applications of Hyperpolarized Metabolism. *American Journal of Neuroradiology* **2010**, *31*, 24–33.
(26) Chekmenev, E. Y.; Hövener, J.; Norton, V. A.; Harris, K.; Batchelder, L. S.; Bhattacharya, P.; Ross, B. D.; Weitekamp, D. P. PASADENA Hyperpolarization of Succinic Acid for MRI and NMR Spectroscopy. *J. Am. Chem. Soc.* **2008**, *130*, 4212–4213, PMID: 18335934.
(27) Bhattacharya, P.; Chekmenev, E. Y.; Perman, W. H.; Harris, K. C.; Lin, A. P.; Norton, V. A.; Tan, C. T.; Ross, B. D.; Weitekamp, D. P. Towards hyperpolarized 13C-succinate imaging of brain cancer. *Journal of Magnetic Resonance* **2007**, *186*, 150–155.
(28) Zacharias, N. M.; Chan, H. R.; Sailasuta, N.; Ross, B. D.; Bhattacharya, P. Real-Time Molecular Imaging of Tricarboxylic Acid Cycle Metabolism in Vivo by Hyperpolarized 1-13C Diethyl Succinate. *J. Am. Chem. Soc.* **2012**, *134*, 934–943, PMID: 22146049.
(29) Berner, S.; Schmidt, A. B.; Ellermann, F.; Korchak, S.; Chekmenev, E. Y.; Glöggler, S.; von Elverfeldt, D.; Hennig, J.; Hövener, J.-B. High field parahydrogen induced polarization of succinate and phospholactate. *Phys. Chem. Chem. Phys.* **2021**, *23*, 2320–2330.
(30) Dagys, L.; Bengs, C.; Moustafa, G. A. I.; Levitt, M. H. Deuteron-Decoupled Singlet NMR in Low Magnetic Fields: Application to the Hyperpolarization of Succinic Acid. *ChemPhysChem* **2022**, *23*, e202200274.
(31) Reineri, F.; Viale, A.; Ellena, S.; Boi, T.; Daniele, V.; Gobetto, R.; Aime, S. Use of Labile Precursors for the Generation of Hyperpolarized Molecules from Hydrogenation with Parahydrogen and Aqueous-Phase Extraction. *Angewandte Chemie International Edition* **2011**, *50*, 7350–7353.
(32) Kovtunov, K.; Beck, I.; Bukhtiyarov, V.; Koptyug, I. Observation of Parahydrogen-Induced Polarization in Heterogeneous Hydrogenation on Supported Metal Catalysts. *Angewandte Chemie International Edition* **2008**, *47*, 1492–1495.
(33) Kovtunov, K. V.; Salnikov, O. G.; Skovpin, I. V.; Chukanov, N. V.; Burueva, D. B.; Koptyug, I. V. Catalytic hydrogenation with parahydrogen: a bridge from homogeneous to heterogeneous catalysis. *Pure and Applied Chemistry* **2020**, *92*, 1029–1046.
(34) Pokochueva, E. V.; Burueva, D. B.; Salnikov, O. G.; Koptyug, I. V. Heterogeneous Catalysis and Parahydrogen-Induced Polarization. *ChemPhysChem* **2021**, *22*, 1421–1440.
(35) McCormick, J.; Korchak, S.; Mamone, S.; Ertas, Y. N.; Liu, Z.; Verlinsky, L.; Wagner, S.; Glöggler, S.; Bouchard, L.-S. More than 12% polarization and 20 minute lifetime of 15N in a choline derivative utilizing parahydrogen and a rhodium nanocatalyst in water. *Angewandte Chemie* **2018**, *130*, 10852–10856.
(36) Glöggler, S.; Grunfeld, A. M.; Ertas, Y. N.; McCormick, J.; Wagner, S.; Schleker, P. P. M.; Bouchard, L.-S. A nanoparticle catalyst for heterogeneous phase para-hydrogen-induced polarization in water. *Angewandte Chemie International Edition* **2015**, *54*, 2452–2456.
(37) Zhivonitko, V. V.; Kovtunov, K. V.; Beck, I. E.; Ayupov, A. B.; Bukhtiyarov, V. I.; Koptyug, I. V. Role of Different Active Sites in Heterogeneous Alkene Hydrogenation on Platinum Catalysts Revealed by Means of Parahydrogen-Induced Polarization. *The Journal of Physical Chemistry C* **2011**, *115*, 13386–13391.
(38) Corma, A.; Salnikov, O. G.; Barskiy, D. A.; Kovtunov, K. V.; Koptyug, I. V. Single-Atom Gold Catalysis in the Context of Developments in Parahydrogen-Induced Polarization. *Chemistry – A European Journal* **2015**, *21*, 7012–7015.
(39) Skovpin, I. V.; Kovtunova, L. M.; Nartova, A. V.; Kvon, R. I.; Bukhtiyarov, V. I.; Koptyug, I. V. Anchored complexes of rhodium and iridium for the hydrogenation of alkynes and olefins with parahydrogen. *Catal. Sci. Technol.* **2022**, *12*, 3247–3253.
(40) Gierse, M. et al. Parahydrogen-Polarized Fumarate for Preclinical in Vivo Metabolic Magnetic Resonance Imaging. *J. Am. Chem. Soc.* **2023**, *145*, 5960–5969, PMID: 36857421.
(41) Wilson, D. M.; Keshari, K. R.; Larson, P. E.; Chen, A. P.; Hu, S.; Van Criekinge, M.; Bok, R.; Nelson, S. J.; Macdonald, J. M.; Vigneron, D. B., et al. Multi-compound polarization by DNP allows simultaneous assessment of multiple enzymatic activities in vivo. *Journal of magnetic resonance* **2010**, *205*, 141–147.
(42) Billingsley, K. L.; Josan, S.; Park, J. M.; Tee, S. S.; Spielman-Sun, E.; Hurd, R.; Mayer, D.; Spielman, D. Hyperpolarized [1,4-13C]-diethylsuccinate: a potential DNP substrate for in vivo metabolic imaging. *NMR in Biomedicine* **2014**, *27*, 356–362.

Acknowledgement This project has received funding from the European Union's Horizon 2020 Research and Innovation Programme under the Marie Skłodowska-Curie Grant Agreement 766402 and the DFG (Project ID 465084791), from the Spanish Ministry under projects MCIN/AEI/10.13039/501100011033 (Ref. PID2020-117859RA-I00 and RYC2020-029099-I), by "ESF Investing in your future", the European Union's Horizon 2020 research and innovation program (GA-863037), and the BIST – "la Caixa" initiative in Chemical Biology (CHEMBIO). J.E. was supported in part by a Fundació Bosch Aymerich (FBA) fellowship through the Barcelona Institute of Science and Technology, and Marie Skłodowska-Curie grant agreement No. 101063517. I.V.K. and D.B.B. thank the Russian Science Foundation (Grant #22-43-04426) for financial support of this work. We thank Giorgio Fusi and Sjoerd Engels for providing chemicals used in this work.